European Journal of Applied Sciences – Vol. 13, No. 02
Publication Date: April 25, 2025
DOI:10.14738/aivp.1302.18595.
Yang, C.-C., Peng, J.-S., Duan, Y.-S., & Sung, C.-L. (2025). The Numerical Study of Multi-Stage Cold Forming Process for the Manufacture of SCM435 Alloy Steel Flange Nuts. European Journal of Applied Sciences, Vol - 13(02). 400-411.

The Numerical Study of Multi-Stage Cold Forming Process for the Manufacture of SCM435 Alloy Steel Flange Nuts

Chih-Cheng Yang
Department of Mechanical and Automation Engineering,
Taiwan Steel University, Taiwan

Jun-Shuo Peng
Graduate School of Mechatronic Science and Technology,
Taiwan Steel University, Taiwan

Yan-Siang Duan
Graduate School of Mechatronic Science and Technology,
Taiwan Steel University, Taiwan

Chen-Lun Sung
Graduate School of Mechatronic Science and Technology,
Taiwan Steel University, Taiwan

ABSTRACT

In this study, a multi-stage cold forming process for flange nut manufacturing using SCM435 alloy steel is numerically investigated. The cold forming process through five stages includes flattening along with centering, upsetting a hexagonal shape along with backward extrusion, upsetting a flange along with backward extrusion, and piercing. The numerical study of cold forming is conducted using the finite element code of DEFORM-3D. The formability of the workpiece is studied, such as the influence on forming force responses, maximum forming forces, effective stress and strain distributions and metal flow pattern. In the five-stage forming process, for the forming stages of upsetting along with backward extrusion and piercing, due to large deformation, the effective stresses in the workpiece are significantly high, and so the effective strains. The flow line distributions are also very complex, where the flow lines in the piercing region around the inner wall of the hole are severely bent, highly compacted, and eventually fractured. For the maximum axial forming force, the first stage of flattening and centering for backward extrusion is 368.5 kN, which is the largest among the five stages, while the forming energy of 183.3 J is the smallest due to shorter acted axial forming stroke. For the forming energy, the second stage, which the workpiece is upset into a hexagonal shape along with backward extruded into a cavity; and the third stage, which the workpiece is upset into a flange along with backward extruded into a cavity, are respectively 456.7 J and 455.7 J that are very close, which are the first and second largest forming energy among the five stages due to longer acted axial forming strokes. The total maximum axial forming force from the first to the last stages is 1,061.4 kN and the total forming energy is about 1.637 kJ.

Keywords: cold forming, flange nut, formability, forming force, effective stress, effective strain.

1. INTRODUCTION

Cold forging is a forming process conducted at room temperature, widely used in many industries, particularly in the manufacturing of fasteners and special parts. Multi-stage cold forging is extensively employed to produce various part products, such as screws, bolts, nuts, rivets, and special fasteners [1]. The SCM 435 alloy steel flange nuts are high-strength fasteners widely used in critical applications. The cold forging process involves mechanical considerations and is influenced by material properties. In cold forging, the tools are subjected to relatively high stresses. Predicting forming loads and stresses is crucial for die design and machine selection. The strain distribution at each forming stage is critical, as it determines the hardness distribution and formability of the part [2].

Numerical simulations are widely applied in many cold forming applications to predict and analyze forming designs. Altan and Knoerr [3] employed the two-dimensional finite element method to investigate suck-in type extrusion defects, bevel gear forging, stress analysis of forging tools and multi-stage cold forging designs. Lee et al. [4] utilized the rigid-plastic finite element method to design the process sequence of multi-stage cold forging for forming constant-velocity joint housing with shaft. They investigated velocity distributions, effective strain distributions, and forging loads, which are useful information in process design. Joun et al. [5] proposed a numerical simulation technique for the forging process involving spring-attached die. They employed a penalty rigid-plastic finite element method in conjunction with an iterative force-balancing method. They investigated significance of metal flow lines for quality control, as well as the effects of spring-attached dies on the metal flow lines and the reduction of forming load. Roque and Button [6] utilized ANSYS, a commercial general finite element software, to simulate forming operations. They developed models to simulate the ring compression test and upsetting operation which was a stage in the manufacturing process of automotive starter components. McCormack and Monaghan [7] numerically analyzed the cold-forging process of a hexagonal head bolt using the finite-element analysis code of DEFORM. The finite element analysis revealed that the highest stress concentration occurred within the tool body, rather than along the contact surface.

MacCormack and Monaghan [8] proposed a three-stage cold forging process for forming a spline shape on the head of an aerospace fastener. They gained insight into the operation by numerically analyzing the strain, damage, and flow patterns for all three stages. Cho et al. [9] conducted a numerical study on the process design of axisymmetric parts in forward and backward extrusion during cold forging operations. The numerical simulation results were in good agreement with the experimental results. Hu and Wang [10] developed a multi-stage upsetting method to form a thick and wide flange at the pipe end. They analyzed simulation results and discussed the method of determining the step-length. To analyze the formability of the multi-stage forging process, Park et al. [11] applied the finite element method to establish a systematic process analysis method for the multi-stage forming of a constant velocity joint outer race. Farhoumand and Ebrahimi [12] utilized the FE code of ABAQUS to analyze the forward-backward-radial extrusion process and to investigate the influence of geometric parameters such as die corner radius and gap height as well as process conditions such as friction on the process. The numerical results were compared with experimental data in terms of forming loads and material flow in different regions. The hardness distribution of the longitudinal section of the product was used to verify the strain distribution obtained from

the numerical analysis. Ji et al. [13] utilized DEFORM_2D numerical code to study the cold forming mechanism of a five-stage cold extrusion process of shaft parts used in gearboxes. The results revealed that the five-stage cold extrusion process is feasible and the forming rules were obtained.

Paćko et al. [14] presented an application of finite element analysis in the prediction and optimization of bolt forming process. The investigated bolt forming process consisted of six stages including cutting, three upsetting stages, backward extrusion, and trimming. Several tool modifications were proposed and analyzed using numerical simulation. Yang and Lin [15] conducted numerical and experimental studies on two forming modes for two-step forward extrusion forming of AISI 1010 carbon steel. The numerical results for the effective strain distributions are consistent with the experimentally measured hardness distribution. Ku [16] proposed a two-stage cold forging process for manufacturing AISI 1035 steel drive shafts with internal spline and spur gear geometry. The process primarily involved a forward extrusion for preform and a forward-backward extrusion for the drive shaft. The preform and the drive shaft produced by the two-stage cold forging experiments were compared with the required target and the numerically predicted configurations. The results demonstrated that the proposed two-stage cold forging process could be well applied to the production of the drive shaft with internal spline and spur gear structures. Francy et al. [17] used finite element code of DEFORM-3D and Taguchi method to optimize the input process parameters in the extrusion process. The simulations were performed by DFORM-3D software to anticipate the minimum force achieved in cold forward extrusion process. Winiarski et al. [18] used DEFORM 2D/3D to numerically study the six-stage cold forging process of 42CrMo4 steel hollow flanged parts to determine whether the proposed forging technique could be used to produce hollow flanged parts.

Jo et al. [19] developed a multi-stage cold forging process using finite element analysis to manufacture a high-strength one-body input shaft with a long body and no separate components. This study provided a proof-of-concept for the design and development of a multi-stage cold forging process to manufacture a one-body input shaft with improved mechanical properties and material recovery. Lee et al. [20] proposed the use of a multi-stage cold forging process to reduce the manufacturing cost of the solenoid valve while satisfying dimensional accuracy and performance. The forming process was divided into six stages to improve the dimensional accuracy of the armature outer diameter, full length and slot part. The dimensional accuracy of the test product was improved through the proposed multi-stage cold forging process design. Yang and Liu [21] conducted numerical and experimental investigations on a five-stage cold forming process for manufacturing low carbon steel AISI 1010 relief valve regulating nuts. The numerical simulation and experimental results had good consistency in the growth trend of the forming force. The effective strain distributions were consistent with the measured hardness distributions. The highly compact grain flow lines also led to higher hardness.

Yang et al. [22] conducted a numerical study on the multi-stage cold forming process of SCM440 alloy steel hexagonal head flange bolts. The cold forming process through five stages included forward extrusion, two upsetting operations, hexagonal trimming and circular trimming. The effective stresses in the head of the workpiece were significantly high, and the

effective strains are also significantly high due to large deformation. The flow line distributions were very complex, where the flow lines in the trimming region of the upset head were severely bent, highly compacted, and eventually fractured due to excessive trimming. Yang et al. [23] conducted a numerical analysis on a three-stage cold forming process for the manufacture of AISI 316 stainless steel Allen screws and hexalobular socket screws. In the three-stage forming process, including two upsetting and one backward extrusion operations, the effective stresses in the head of the workpiece were significantly high, and the effective strains were also significantly high due to large deformation. Kim et al. [24] experimentally investigated the strain hardening, elongation, and shearing speed effects of flow behaviors on coil-rod shearing during automatic multi-stage cold forging. Various coil materials were tested, including A6061-T6, SWCH10A, SCM435 and SCM415. The new findings revealed that the coil-rod shearing phenomena and surface features were strongly dependent on flow behaviors and shearing speed. They could lead the engineers to design an optimized shearing process. Winiarski et al. [25] proposed a new method to form flanges in hollow parts. The process involved an extrusion using two dies which moved in the opposite direction to that of the punches. This particular kinematics of the tools made it possible to form two flanges simultaneously in one tool pass.

In this study, the numerical simulation of a five-stage cold-forming process for the manufacture of SCM435 alloy steel flange nuts is presented. The forming process includes flattening and centering, upsetting into a hexagonal shape along with backward extrusion, upsetting into a flange along with backward extrusion, and piercing. The numerical simulation of cold forming is conducted using the finite element code of DEFORM-3D. The forming load responses are calculated and the effective stress, effective strain and metal flow pattern at various deformation zones are studied.

2. MATERIALS AND METHODS

The manufacturing process of the flange nuts is a multi-stage cold forming through five stages. The actual forming machine has five-stage close die. A cold-forging quality SCM435 alloy steel wire coil, which is fabricated by China Steel Corporation, Kaohsiung, Taiwan, is used in the cold-forming analysis. The chemical composition of the alloy steel wire is shown in Table 1.

Table 1: Chemical composition of SCM435 alloy steel wires (wt.%).

C	P	Mn	Si	Al	Cu	Ni	Cr	Mo
0.37	0.014	0.74	0.21	0.048	0.007	0.01	0.99	0.17

The numerical study of cold forming is conducted using the finite element code of DEFORM-3D. A billet of ϕ14.0mm × L14.9mm is cut by the shearing die and transfer to forming stations. The three-dimensional and cross-section views for initial billet and product parts of five stages are shown in Figure 1.

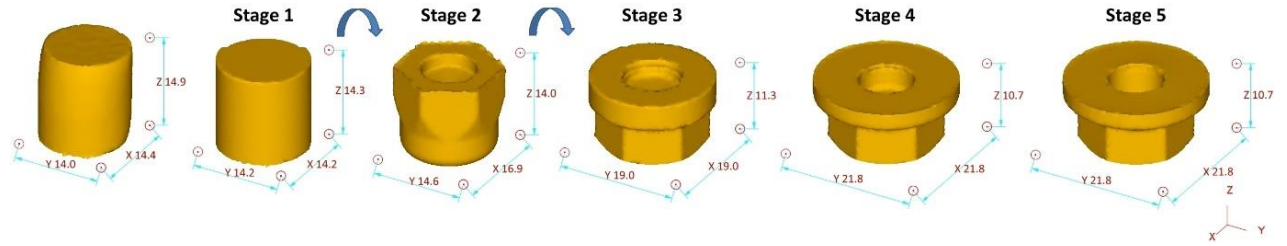

(a) 3D views

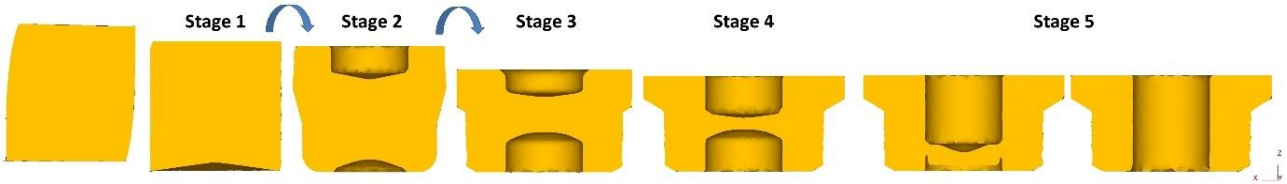

(b) cross-section views

Figure 1: The shapes for initial billet and product parts of each stage.

Flange nut is a short part, and the initial billet to be formed is also comparatively short. The sheared billet is obviously asymmetrical, as shown in Figure 1. Therefore, it is usually necessary to flatten the sheared billet with one stage. To obtain more accurate simulation results, without any assumption of symmetry, the billet is pre-sheared numerically. Due to cutting to length by shearing, both the ends of the cutoff billet are visibly deformed, as shown in Figure 1. The initial billet is obviously not an axisymmetric cylindrical body. In the first stage, as shown in Figures 1(a) and 1(b), the process includes flattening the billet end and centering for the backward extrusion in the second stage, then it is turned over by a transfer mechanism and moved to the second stage in which the upper end of the workpiece is upset into a hexagonal shape and simultaneously backward extrusion process is carried out over a moving punch to form a cavity, as shown in Figures 1(a) and 1(b). In the third stage, the workpiece is turned over again to upset into a flange of ϕ19.0 mm and simultaneously a cavity of ϕ8.4 mm is backward extruded at the top end to a depth of 2.4 mm by using a moving punch. Subsequently, the workpiece is moved to the fourth stage, wherein the flange of the workpiece is further upset to an outer diameter of ϕ21.8 mm, while simultaneously, the cavity is further backward-extruded to a depth of 3.9 mm. Finally, it moved to the fifth stage, wherein the inner hole is formed by piercing. The deformation energy is

$$E = \int_0^{\Delta L} F dl \tag{1}$$

where F is forming force and ΔL is total acted forging stroke.

The numerical simulations of multi-stage cold forming are constructed as a 3D finite element analysis using DEFORM 3D. The workpiece is modeled using tetrahedral elements. The deformations of punches and dies are ignored and considered as rigid objects because their materials are generally much harder than the material of workpiece. The workpiece material is a SCM 435 alloy steel billet which is considered as a rigid-plastic material with Von Misses yield criterion, isotropic hardening. In order to obtain more accurate simulation results, a cylindrical compression test, with the specimens of ϕ8.35mm × L11.4mm, is conducted in a

20 tonne universal testing machine under a constant ram speed of 3 mm/min at room temperature, and the following equations are used to gain the true stress and true strain [26],

$$\sigma = P/A_0, \tag{2}$$

$$\varepsilon = (h - h_0)/h_0, \tag{3}$$

$$\sigma_t = \sigma\,(1 + \varepsilon) = \sigma\,(h/h_0), \tag{4}$$

$$\varepsilon_t = \ln(1 + \varepsilon) = \ln(h/h_0), \tag{5}$$

where σ is engineering stress, ε is engineering strain, P is compression force, A_0 is initial cross-sectional area, h_0 is initial height, h is the instantaneous height, σ_t is true stress and ε_t is true strain. Figure 2 demonstrates the compression true stress-true strain diagram of SCM 435 alloy steel, which will be imported into the numerical code of DEFORM to conduct the forming simulation analysis.

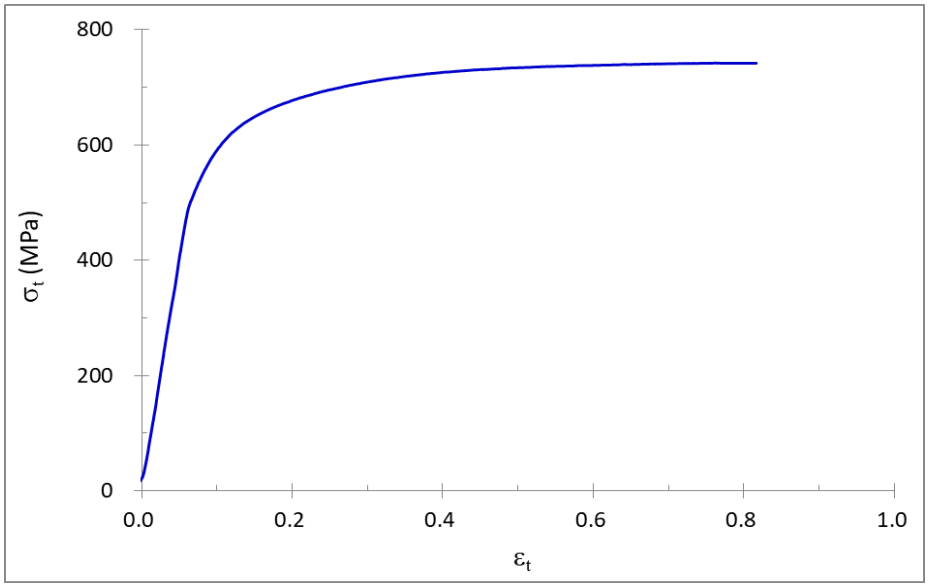

Figure 2: True stress-true train curve of SCM435 alloy steel by compression test.

The friction between the workpiece and tools is considered as constant shear friction, and the friction coefficient for cold forming is m = 0.12. The relevant simulation settings are listed in Table 2.

Table 2: Simulation settings in the FE code of DEFORM.

Workpiece material	**SCM 435**
Workpiece/die property	Plastic/rigid
Temperature	20°C
Mesh number	32,000
Mesh element type	Tetrahedron
Friction model/friction coefficient	Constant shear friction/0.12

3. COLD FORMING OF FLANGE NUTS

For the multi-stage cold forming of flange nuts through five stages, the effect of forging load response, maximum forging load, effective stress and effective strain distributions, and metal flow pattern are studied numerically.

3.1 The Forming Load Response and Deformation Energy

The five-stage forming simulation results are shown in Figure 3 for the axial forces. The maximum forming forces are indicated for each stage. The axial forming stroke (ΔL) and deformation energy (E) for each stage are shown in Table 3.

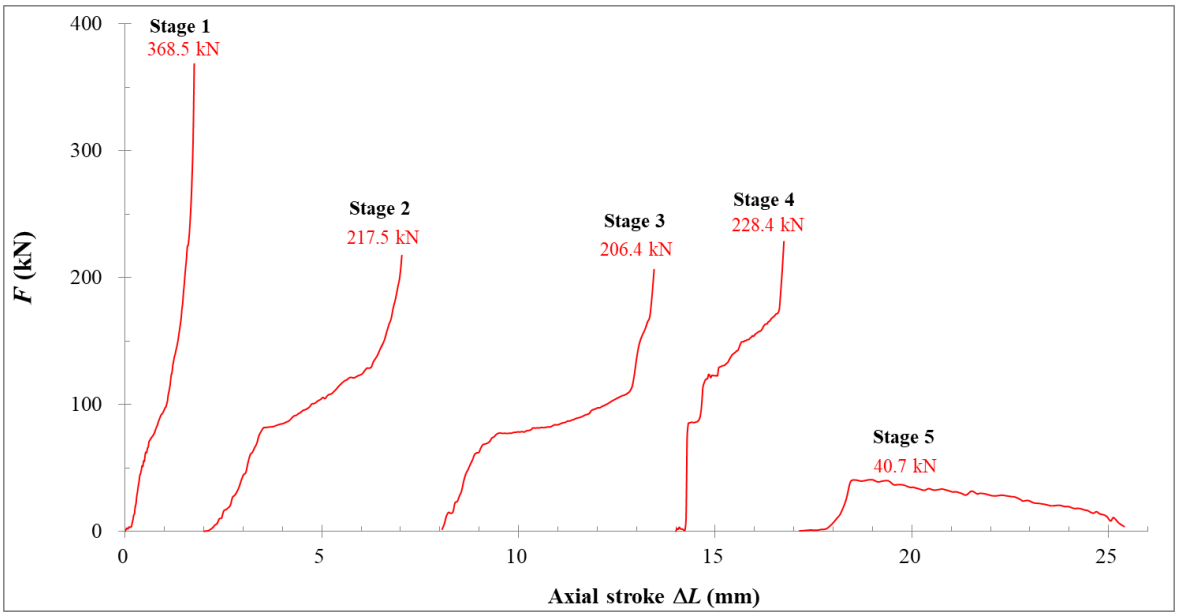

Figure 3: Axial Forging responses for five-stage forming.

From the force responses of the forming force in the five stages, it is observed that at first stage the maximum axial forming force is 368.5 kN, which is the greatest of the five stages as shown in Figure 3, and there is only a minor deformation to remove the sharp cutting edges and to center for the backward extrusion. Thus, the acted axial forging stroke is only 1.76 mm and the forming energy is 183.3 J due to shorter acted axial forming stroke, as shown in Table 3. In the second stage, the maximum forming force is 217.5 kN to upset the upper end of the workpiece into a hexagonal shape and simultaneously to backward extrude over a moving punch to form a cavity, as shown in Figure 1. The acted axial forging stroke is 5.03 mm and the forming energy is 456.7 J, for a longer acted axial forming stroke of 5.03 mm, as shown in Table 3. In the third stage, the workpiece is upset into a flange with a diameter of ϕ19.0 mm, while simultaneously a cavity is formed at the top via backward extrusion over a moving punch. The forming force reaches a maximum value of 206.4 kN, as shown in Figure 3. The forming process in this stage is similar to that of the second stage, and the forming energy of 455.7 J, which is very close to the forming energy of the second stage but higher than that of the first stage, as shown in Table 3. In the fourth stage, to further upset the flange to a larger outer diameter of ϕ21.8 mm while simultaneously further backward-extruding the cavity to a depth of 3.9 mm, the maximum axial forming force is 228.4 kN, which is greater than the

forming forces in the second and third stages, while the forming energy of 342.1 J is less than the forming energy in the second and third stages but greater than the forming energy in the first stage, as shown in Table 3. In the final stage, a hole is pierced in the workpiece cavity with a maximum axial forming force of 40.7 kN, the smallest among the five stages, as illustrated in Figure 3. The forming energy is 199.5 J, lower than that of the second, third, and fourth stages, as shown in Table 3. Overall, the total maximum axial forming force from the first to the final stages is 1,061.4 kN, and the total forming energy is approximately 1.637 kJ.

Table 3: The acted axial forging stroke (ΔL) and deformation energy (E) for each stage.

Stage	1	2	3	4	5	Total
E (J)	183.3	456.7	455.7	342.1	199.5	1,637.2
ΔL (mm)	1.76	5.03	5.45	2.75	8.40	

3.2 The Effective Stress Analysis

The effective stress distributions are shown in Figure 4 at the final position of each stage for the five-stage forming, and the maximum effective stresses are indicated. In the first stage, stresses are arising at the upper and lower ends of workpiece when they are in contact with the dies, then the stresses increase as the forging load increases, the maximum effective stress is 759 MPa. It is observed that the highest value of effective stress occurs in the upper and lower ends whereas the lower value of effective stress occurs in the middle region of workpiece. For the second stage, which involves upsetting the upper end of the workpiece into a hexagonal shape along with backward extrusion over a moving punch to form a cavity, it is analyzed from Figure 4 that the effective stresses are high in the upsetting and extrusion deformation region. This results in the formation of a hexagonal head and a cavity at upper face under high pressure in turn causes high effective stress of 762 MPa on workpiece and tool surface. The stress response in the backward extrusion and upsetting region of workpiece is obviously larger, as shown in Figure 4. For the third stage which involves upsetting into a flange of ϕ19.0 mm along with backward extruding a cavity at the top end over a moving punch, stresses are arising in the whole workpiece when they are in contact with the dies, then the stresses increase as the forming load increases, as shown in Figure 4, the maximum effective stress is 761 MPa. It is observed that the highest value of effective stress occurs in the whole workpiece.

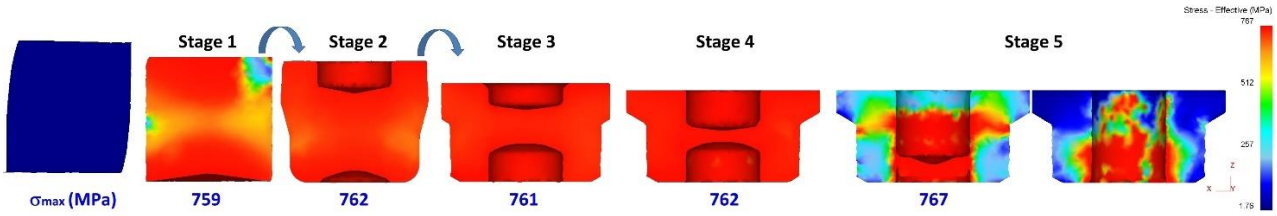

Figure 4: The effective stress distributions at the final position of each stage.

In the fourth stage, the flange of the workpiece is further upset to a larger outer diameter of ϕ21.8 mm and simultaneously further backward-extruded the cavity to a depth of 3.9 mm. This results in the formation of the larger flange and the deeper cavity in the upper face being under high pressure and results in a highly effective stress of 762 MPa, as shown in Figure 4.

The stress response of the entire workpiece is obviously large. In the fifth stage, the process of piercing over a piercing punch is carried on to form a hole in the inner cavity. Therefore, the stress response is relatively large in the piercing zone of the workpiece, as shown in Figure 4, and results in high effective stress of 767 MPa.

3.3 The Effective Strain Analysis

The effective strain distributions at the final position for the five stages are shown in Figure 5. In the first stage, the effective strains in flatting (upper) and centering (lower) regions of workpiece are higher than the middle region where the deformation is small, as illustrated in Figure 5. The effective strain distributions are not perfectly symmetric due to the visible deformation at the ends of the cutoff billet. For the second stage of upsetting the upper end of the workpiece into a hexagonal shape along with backward extrusion over a moving punch to form a cavity, the effective strains are high in the extrusion and upsetting deformation region with large deformation, as shown in Figure 5. Due to the friction resistance on the contact surface between the tool and the workpiece, the effective strains along the tool region are obviously high. For the third stage of upsetting into a flange of ϕ19.0 mm along with backward extruding a cavity at the top end over a moving punch, the effective strains are high in the upsetting and extruding region with large deformation and in the end region of cavities compression over extruding tools, as shown in Figure 5. For the fourth stage of further upsetting to a larger flange along with further backward-extrusion to a deeper cavity, the effective strains are obviously high in the upsetting face and extruding region and the end region of cavities compression over extruding tools, while the effective strains of the other region are relatively small, as shown in Figure 5. However, even though the first four stages are axisymmetric forming, their effective strain distributions are obviously not axisymmetric, as shown in Figure 5, since the initial billet is not an axisymmetric cylindrical body. In the fifth stage, the process of piercing over a moving punch is conducted to pierce a hole in internal cavity and the highly effective strains are obviously distributed in the inner wall of the hole and the piercing waste, as shown in Figure 5.

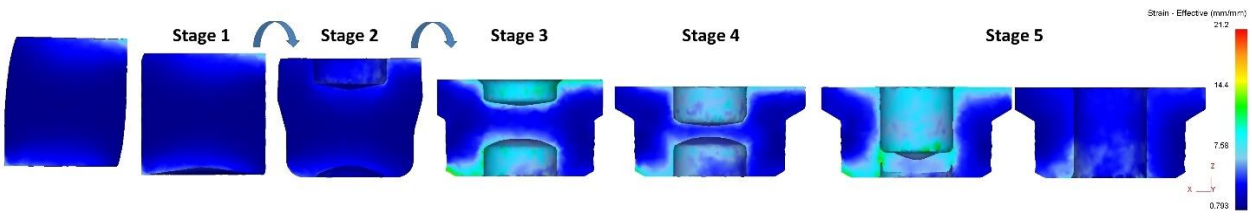

Figure 5: The effective strain distributions at the final position of each stage.

3.4 The Flow Line Analysis

When the metal is deformed by cold forming, the deformed grains and inclusions in the metal are distributed in bands along the main deformation direction of the metal, formed the grain flow lines. The simulation results of flow lines for the five-stage forming are shown in Figure 6. The flow lines in the initial billet are obviously not axisymmetric either evenly distributed, as shown in Figure 6. The flow lines in the sheared ends are vertically bent and highly compacted due to shear deformation. The highly compacted are the flow lines, the higher is the hardness [21].

In the first stage, the flow lines in flatting (upper) and centering (lower) regions of workpiece are highly compacted, while in the middle region with low deformation, the flow lines are almost evenly distributed. For the second stage of upsetting the upper end of the workpiece into a hexagonal shape along with backward extrusion over a moving punch to form a cavity, the flow lines in the inner wall of the upper cavity are obviously highly compacted, as shown in Figure 6, because of severe structure deformation. For the third stage of upsetting into a flange of ϕ19.0 mm along with backward extruding a cavity at the top end over a moving punch, the flow lines in the upsetting and extruding region with large deformation and in the end region of cavities compression over extruding tools are curved and highly compacted, as shown in Figure 6. For the fourth stage of further upsetting to a larger flange along with further backward-extrusion to a deeper cavity, the flow lines in the upsetting face and extruding region and the end region of cavities compression over extruding tools are severely curved and those in the end region of cavities are more highly compacted, as shown in Figure 6.

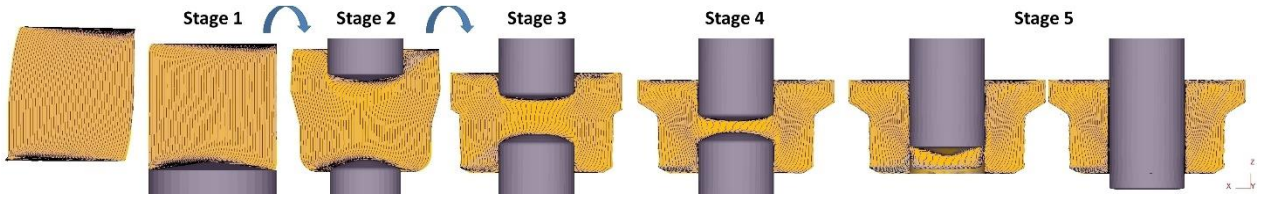

Figure 6: The simulation results of flow lines at the final position of each stage.

For the fifth stage of piercing a hole in internal cavity over a moving punch, the flow lines around the inner wall of the hole are severely curved, deformed severely and more highly compacted and eventually break, as shown in Figure 6.

4. CONCLUSIONS

A multi-stage cold forming process for the manufacture of flange nuts is numerically studied with SCM435 alloy steel. The cold forming process through five stages includes flattening and centering for backward extrusion, upsetting a hexagonal shape along with backward extrusion over a moving punch, upsetting a flange along with backward extrusion over a moving punch, and piercing. The numerical simulations of cold forming are carried out using the FE code of DEFORM-3D. The formability of the workpiece is studied, such as the effect on forming load response, maximum forming force, effective stress and strain distributions, and metal flow pattern.

For the maximum axial forming force, the first stage of flattening and centering for backward extrusion is 368.5 kN, which is the largest among the five stages, while the forming energy of 183.3 J is the smallest due to shorter acted axial forming stroke. For the forming energy, the second stage, which the workpiece is upset into a hexagonal shape along with backward extruded into a cavity; and the third stage, which the workpiece is upset into a flange along with backward extruded into a cavity, are respectively 456.7 J and 455.7 J that are very close, which are the first and second largest forming energy among the five stages due to longer acted axial forming strokes. Overall, the total maximum axial forming force from the first to the last stages is 1,061.4 kN and the total forming energy is about 1.637 kJ.

In the five-stage forming process, for the forming stages of upsetting along with backward extrusion and piercing, the effective stresses in the workpiece are significantly high, and the effective strains are also significantly high due to large deformation. In particular, the maximum effective stress in the fifth stage, the process of piercing to form a hole, is 767 MPa, which is the largest among the five stages. The flow line distributions are also very complex in which the flow lines in the piercing region around the inner wall of the hole are severely bent, highly compacted, and eventually fractured. However, even though the five stages are axisymmetric forming, their effective strain and flow line distributions are obviously not axisymmetric since the initial billet is not an axisymmetric cylindrical body.

References

[1] Sevenler, K.; Raghupati, P.S.; Altan, T., Forming Sequence Design for Multi-stage Cold Forging. Journal of Mechanical Working Technology, 1987. 14(2): p.121-135.

[2] Kobayashi, S.; Oh, S.-I; Altan, T., Metal forming and the Finite-element Method, Oxford University, England, 1989.

[3] Altan, T. and Knoerr, M., Application of the 2D Finite Element Method to Simulation of Cold Forging Processes. Journal of Materials Processing Technology, 1992. 35: p.275-302.

[4] Lee, J.-H.; Kang, B.-S.; Lee, J.-H., Process design in multi-stage cold forging by the finite-element method. Journal of Materials Processing Technology, 1996. 58(2-3): p.174-183.

[5] Joun, M.S.; Lee, S.W.; Chung, J.H., Finite element analysis of a multi-stage axisymmetric forging process. International Journal of Machine Tools and Manufacture, 1998. 38: p. 843-854.

[6] Roque, C.M.O.L. and Button, S.T., Application of the finite element method in cold forging processes. Journal of the Brazilian Society of Mechanical Sciences, 2000. 22(2): p.189-202.

[7] McCormack, C. and Monaghan, J., A finite element analysis of cold-forging dies using two- and three-dimensional models. Journal of Materials Processing Technology, 2001. 118(1-3): p.286-292.

[8] MacCormack, C. and Monaghan, J., 2D and 3D finite element analysis of a three stage forging sequence. Journal of Materials Processing Technology, 2002. 127: p.48-56.

[9] Cho, H.Y.; Min, G.S.; Jo, C.Y.; Kim, M.H., Process design of the cold forging of a billet by forward and backward extrusion. Journal of Materials Processing Technology, 2003. 135(2-3): p.375-381.

[10] Hu, X.L. and Wang, Z.R., Numerical simulation and experimental study on the multi-step upsetting of a thick and wide flange on the end of a pipe. Journal of Materials Processing Technology, 2004. 151(1-3): p.321-327.

[11] Park, K.S.; VanTyne, C.J.; Moon, Y.H., Process analysis of multistage forging by using finite element method. Journal of Materials Processing Technology, 2007. 187-188: p.586-590.

[12] Farhoumand, A. and Ebrahimi, R., Analysis of forward–backward-radial extrusion process. Materials & Design, 2009. 30: p.2152-2157.

[13] Ji, D.S.; Jin, J.S.; Ma, W.J.; Xia, J.C.; Xia, H.G.; Dong, Y., Multistage Cold Extrusion Process and Forming Rules of Shaft Parts Used in Gearbox. Advanced Materials Research, 2010. 148-149: p.683-687.

[14] Paćko, M.; Sleboda, T.; Macioł, S.; Packo, P., Optimization of a Bolt Forming Process by Means of Numerical Simulation. Steel Research International, 2012.

[15] Yang, C.-C. and Lin, X.-Y., The Forming Analysis of Two-stage Extrusion for 1010 Fastener. Journal of Mechanical Engineering and Automation, 2016. 6: p.43-45.

[16] Ku, T.-W., A Study on Two-Stage Cold Forging for a Drive Shaft with Internal Spline and Spur Gear Geometries. Metals, 2018. 8(11): 953.

[17] Francy, K.A.; Rao, C.S.; Gopalakrishnaiah, P., Optimization of Direct Extrusion Process Parameter on 16MnCr5 and AISI1010 Using DEFORM-3D. Procedia Manufufacturing, 2019. 30: p.498-505.

[18] Winiarski, G.; Bulzak, T.A.; Wójcik, Ł.; Szala, M., Numerical Analysis of a Six Stage Forging Process for Producing Hollow Flanged Parts from Tubular Blanks. Advances in Science and Technology – Research Journal, 2020. 14(1): p.201-208.

[19] Jo, A.R.; Jeong, M.S.; Lee, S.K.; Moon, Y.H.; Hwang, S.K., Multi-Stage Cold Forging Process for Manufacturing a High-Strength One-Body Input Shaft. Materials, 2021. 14(3): 532.

[20] Lee, H.-S.; Park, S.-G.; Hong, M.-P.; Kim, Y.-S., Process design of multi-stage cold forging with small size for ESC solenoid valve parts. Journal of Mechanical Science and Technology, 2022. 36: p.359-370.

[21] Yang, C.-C. and Liu, C.-H., The Study of Multi-Stage Cold Forming Process for the Manufacture of Relief Valve Regulating Nuts. Applied Sciences, 2023. 13(10): 6299.

[22] Yang, C.-C.; Nguyen, H. Q.; Wang, K.-H., The Forming Analysis of SCM440 Alloy Steel Hexagon Head Flange Bolts. European Journal of Applied Sciences, 2023. 11(6): p.1-13.

[23] Yang, C.-C.; Nguyen, T.V.; Andres, J.C., The Cold Forming Analysis of Stainless Steel Socket-Head Screws. European Journal of Applied Sciences, 2023. 11(6): p.225-237.

[24] Kim, K.M.; Ji, S.M.; Lee, S.W.; Hong, S.M.; Joun, M.S., Flow behavior dependence of rod shearing phenomena of various materials in automatic multi-stage cold forging. Journal of Mechanical Science and Technology, 2023. 37: p.139-148.

[25] Winiarski, G.; Gontarz, A.; Skrzat, A.; Wójcik, M.; Wencel, S., Analysis of a New Process for Forming Two Flanges Simultaneously in a Hollow Part by Extrusion with Two Moving Dies. Metals, 2024. 14(6), 612.

[26] Hosford, W.F., Mechanical Behavior of Materials, Cambridge University, NY, USA, 2005.